

Biophysics Lab Course 2012

SMALL SPHERES IN A ONE-BEAM GRADIENT TRAP
Optical tweezers calibration using backfocal-plane detection

*Softmatter Physics
Prof. Josef Käs
Linnéstraße 5
04103 Leipzig*

*Assitants: Dan Strehle Carsten Schuldt
Room 301 Room 301
(97) 32562 (97) 32563
dan.strehle@uni-leipzig.de schuldt@physik.uni-leipzig.de*

Introduction

In 1970 Ashkin demonstrated that dielectric particles can be accelerated by the radiation pressure of a laser beam and trapped by two counter-propagating beams. Sixteen years later he succeeded in trapping particles using a single, highly focused laser beam, a setup that was called *optical tweezers*. Optical tweezers have become a powerful tool, in physics as well as in biology, for manipulating objects as large as $100\mu\text{m}$ and as small as a single atom without mechanical contact. For example, inside biological objects such as cells or cell organelles, small probes can be held, moved and rotated by exertion of forces as small as several pN with optical tweezers. In the case of biological samples, light in the near infrared ($\lambda = 700\text{nm}$ to 1100nm) is used in order to prevent radiation damage, which occur with due to the absorption of water or amino acids.

The list of experiments for which optical tweezers have been used is long and a comprehensive overview of biological applications can be found in reference [1]. The historically older two-beam trap has played a major role in the fields of atom trapping and cooling and has been a prerequisite for the first experimental proof of Bose-Einstein condensation. Both achievements have been honored with a Nobel Prize in recent years. However, in biology, this kind of trap has only recently acquired some importance through its use in deforming cells by optically induced forces. In this context, this setup is also called *optical stretcher*.

Theoretical Background

In general, scattering, i.e. the interaction of light with an object, can be divided into two components. The first is the reflection and refraction at the surface of the particle, the second is the diffraction from the rearrangement of the wavefront after it interacts with the particle. While the radiation pattern due to reflection and refraction emanates from the particle in all directions and depends on the refractive index of the particle, the diffraction pattern is primarily in the forward direction and depends only on the particle geometry. Two different regimes of theoretical approach can be distinguished. They are determined by the ratio of the incident light's wavelength λ to the diameter D of the irradiated particle. In the *ray optics regime*, the particle is very large compared to the wavelength ($D \gg \lambda$), whereas in the *Rayleigh regime* the opposite holds ($D \ll \lambda$). The calculation of optical forces for arbitrary particle sizes $D \approx \lambda$ is nontrivial. For a full arbitrary theory, the solution of Maxwell's equations with the appropriate boundary condition is required [3]. The Lorenz-Mie Theory was the first step in that direction and describes scattering of a plane wave by a spherical particle for arbitrary particle size, refractive index, and wavelength. However, the Lorenz-Mie Theory cannot describe a Gaussian beam, such as that produced by a TEM00 laser, which is a particular point of interest to accurately describe laser-induced forces. The calculation of optical forces of Gaussian beams and arbitrarily shaped objects can be achieved by the Generalized Lorenz-Mie Theory (GLMT).

Rayleigh Regime ($D \ll \lambda$)

In the small particle size limit, the dipole or Rayleigh approximation can be applied. This approximation states that the dielectric sphere can be treated simply as an induced point dipole. The forces a particles expires decompose easily in two different parts.

Gradient Force

The *Lorentz force* \mathbf{F} on a point charge q is well known

$$\mathbf{F}(t) = q(\mathbf{E}(t) + \mathbf{v} \times \mathbf{B}(t)). \quad (1)$$

We omit the second term, since the particle's velocity \mathbf{v} be small and the magnetic field $\mathbf{B}(t)$ compared to the electric field $\mathbf{E}(t)$ of light is small, as well. Providing $\mathbf{E}(t)$ is inhomogeneous, it is expanded at a short distance \mathbf{d} and aborted after the linear term. This is inserted in eq. 1

$$\mathbf{F}(t) = \underbrace{(q\mathbf{d})}_{\mathbf{p}} \nabla \mathbf{E}(t) = \mathbf{p} \nabla \mathbf{E}(t) = \alpha \mathbf{E}(t) \nabla \mathbf{E}(t). \quad (2)$$

The dipole moment \mathbf{p} emerges as a prefactor. Itself is given by the polarizability and the $\mathbf{E}(t)$ field. The unification of the vector identity $\nabla(\mathbf{A}^2) = 2(\mathbf{A} \cdot \nabla)\mathbf{A} + 2\mathbf{A} \times (\nabla \times \mathbf{A})$ and *Faraday's law of induction*, providing a constant magnetic field, yields

$$\mathbf{F}(t) = \frac{\alpha}{2} \nabla \mathbf{E}^2(t). \quad (3)$$

This denotes the force at a particular time t . The overall gradient force acting on the particle is a time average. The electric field vector of light oscillates sinusoidal. Its effective value is $1/\sqrt{2}$ its absolute value. Thus,

$$\mathbf{F}_{\text{grad}} = \langle \mathbf{F} \rangle_t = \frac{\alpha}{4} \nabla |\mathbf{E}|^2. \quad (4)$$

Evaluating the intensity I , i.e. the time average of the light's Poynting vector $\mathbf{S}(t)$, yields $I = |\langle \mathbf{S}(t) \rangle_t| \propto |\mathbf{E}|^2$. We find that the gradient force is proportional to the polarizability α and the gradient (hence the name) of the light's intensity ∇I , i.e. toward the beam axis in case of a Gaussian beam profile, and toward the focus of the laser given the laser is focussed.

Scattering Force

The second significant force stems from the momentum transfer from the impacting photons to the particle. It is the normalized energy flux (Poynting vector) multiplied by the particle's effective cross section σ

$$\mathbf{F}_{\text{scat}} = \frac{n_2}{c} \sigma \langle \mathbf{S} \rangle_t. \quad (5)$$

From above the Poynting vector is already known. Eventually the scattering force is proportional to the cross section σ and the light's intensity in direction of propagation $I \mathbf{e}_z$.

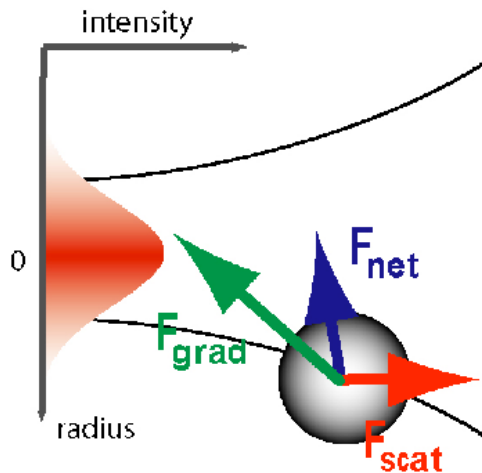


Figure 1: The forces arising for a tightly focused laser beam (Optical Tweezers).

Trapping

A particle displaced from the beam axis experiences the gradient force as a restoring force toward the beam axis. Due to the low curvature of the beam, a component of the gradient force parallel to the direction of light propagation can be neglected. The scattering force due to radiation pressure pushes the particle in the direction of light propagation, i.e., away from the light source. For the trapping of particles, either two counter-propagating beams are required in order for the scattering forces to cancel out (geometry of the two-beam trap or optical stretcher), or a single laser beam has to be focused very tightly.

In a highly focused beam (cf. figure 1), the gradient force possesses a component against the Poynting vector in addition to its component perpendicular to it. This component prevents the particle from being pushed in the direction of light propagation by the scattering force. The net force acts as a restoring force toward the focus of the beam with respect to all three dimensions.

For effective trapping the z component of \mathbf{F}_{grad} has to exceed \mathbf{F}_{scat} in the laser focus significantly.

Ray Optics Regime ($D \gg \lambda$)¹

In the ray optics regime, the size of the object is much larger than the wavelength λ of the light, and a single ray can be tracked throughout the particle. If the ratio of the refractive index of the particle to that of the surrounding medium is not close to one but sufficiently large, diffraction effects can be neglected. This situation is for example given when whole cells, which are microns or tens of microns in size, are trapped using infrared light while suspended in a dilute aqueous solution. The incident laser beam can be decomposed into individual rays with appropriate intensity, momentum, and direction. These rays propagate in a straight line in uniform, nondispersive media and can be

¹Either you have already read this in the Optical Stretcher preparation or you will need it later on.

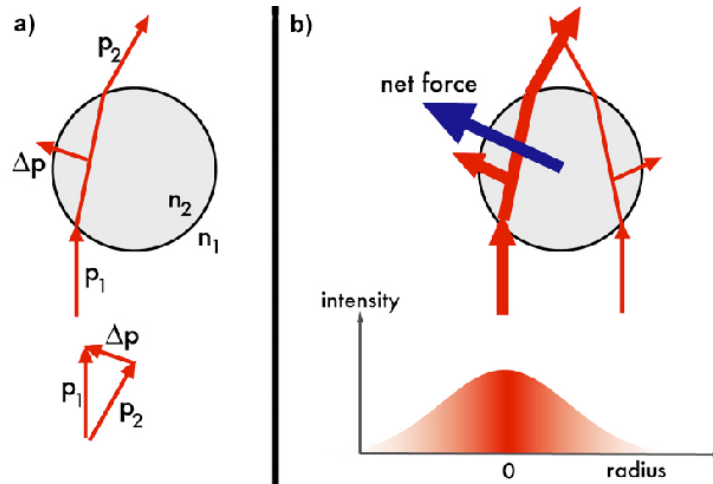


Figure 2: The momenta (red arrows) of (a) one ray and (b) two rays with different intensities propagating through a sphere. The blue arrow indicates the restoring net force.

described by geometrical optics.

Consider a Gaussian laser beam hitting a spherical particle of refractive index n_1 , which is surrounded by a medium of refractive index n_2 (cf. figure 2a). Each incoming ray carries a certain amount of momentum p proportional to its energy E and to the refractive index n_i of the medium it travels in

$$p_i = \frac{n_i}{c} E \quad (6)$$

When the ray penetrated the particle, its momentum has changed in both, direction and magnitude. The momentum difference is carried by the particle. The force due to the directional change of a ray's momentum has components in the longitudinal as well as in the lateral direction. However, there are many rays incident on the particle. The net force has only a forward component due to the rotational symmetry of the problem. This symmetry is broken if the particle is not centered exactly on the optical axis of the Gaussian beam. In this case the particle feels a restoring net force (cf. figure 2b). The net force's component perpendicular to the beam propagation is called the gradient force, its component along the direction of beam propagation the scattering force, in reference to Rayleigh scattering (cf. figure 1). In the ray optics regime, however, these two force-components stem from just one single physical effect as discussed.

Calibration

On the one hand we have a simple qualitative understanding of the physics behind optical trapping, but on the other hand this is not sufficient for calculating the forces exerted on particles for two reasons.

At first, we seize the issue already mentioned before: The particle sizes of about $2\mu\text{m}$ we utilize are in the order of the applied wavelength of $\lambda =$

1064 nm actually. So none of the special cases described above applies. Though several approaches, analytical and numerical, address this regime their outcome is limited since they demand a precise knowledge of a huge set of parameters of the setup.

This leads to the second main question. A lot of the parameters needed for an exact computation of the resulting trap stiffness are difficult to access, i.e. in particular the intensity impinging on the particle.

At last, current ways of calculating the trap stiffness from laser parameters are imprecise. We calibrate the trap empirically by applying a well-characterized signal to the bead and evaluate its response affected by the potential of the focused laser light.

The traditional approaches

An overview concerning the most relevant calibration techniques is given in [1].

Escape force

The underlying principle of the following techniques is the viscous drag exerted by fluid flow. This principle can be applied because a low Reynolds number holds for these micron scaled cases. This means, any inertial forces are negligible and the over damped oscillator is to be described by an external force and a mobility μ or its inverse γ :

$$\mathbf{F} = \frac{1}{\mu} \dot{\mathbf{x}} = \gamma \dot{\mathbf{x}}. \quad (7)$$

In conjunction with knowledge of all parameters of Stokes' Law for a spherical particle,

$$\mathbf{F} = \gamma \mathbf{v} = 6\pi\eta r \mathbf{v}. \quad (8)$$

the maximal force or escape force of an optical trap can be determined by pulling the trapped particle with a progressive velocity through a viscous fluid.

Step Response

Supposing a rapid small displacement within the linear regime of the trap's potential, it will take the particle finite time to return to the potential minimum in the trap center

$$\mathbf{x}_{\text{bead}}(t) = \mathbf{x}_{\text{trap}} (1 - \exp[-\omega_c t]). \quad (9)$$

The relaxation time is $\gamma/\kappa = \omega_c^{-1}$.

Sinusoidal Motion

Contrary to the technique above, the trap position is changed continuously in a oscillating fashion with a drive frequency f_d . By analyzing the parameters of the induced particle's oscillation, the trap stiffness can be derived from the particle's response

$$\mathbf{x}_{\text{bead}}(t) = \frac{\mathbf{x}_{\text{trap}}}{\sqrt{1 + f_c^2/f_d^2}} \exp[-i(2\pi f_d t - \delta)], \quad (10)$$

²Later on we will make extensive use of the corner frequency $f_c = (2\pi)^{-1}\omega_c$

with $f_c = (2\pi)^{-1}\omega_c$ and $\tan \delta = f_c/f_d$ denoting the phase shift of both oscillations. Finally, any anharmonics of the trap potential can be mapped by varying the amplitude of sinusoidal change of the trap position.

Experimental Setup

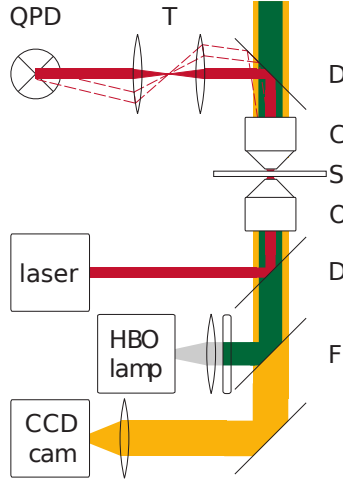


Figure 3: A polarized fiber laser emits coherent light at 1064 nm. A dichroic mirror (**D**) couples the laser beam into the optical path of an inverted microscope. Using a 100x oil immersion objective (**O**) we focus the laser light (**red**) and the fluorescence excitation light (**green**), selected by a filter cube (**F**) from white light, into the sample (**S**). Another objective is employed as a condenser (**C**). Since the position signal is measured by a quadrant photo diode (**QPD**), the significant laser light has to be filtered (**D**) out. Tilted beams are corrected for by a telescope arrangement of two lenses (**T**). The emitted fluorescent light (**yellow**) is observed with a camera (**CCD cam**).

We employ a diode pumped fiber laser at 1064 nm wavelength with a designed power output of 3 W. Several high curvature bends are induced to the polarization maintaining fiber to couple out excess power. The free beam exits the fiber and is collimated to a diameter of 5.4 mm. The non-focused laser beam is coupled into the back focal plane of the objective in an inverted microscope by an adjustable dichroic mirror beneath the objective. A 100x oil objective with high numerical aperture ($NA=1.35$) is used in the experiment. In order to move the sample a coarse manual drive is used in conjunction with a nanometer precise xyz piezo stage. The microscope is ran in brightfield fluorescence mode. Hence, the sample is illuminated at a particular wavelength and images of the sample in the focal plane are taken with a digital CCD camera of the emitted Stokes-shifted photons.

Precise position detection is achieved by mapping the (laser-particle) scattering pattern onto a quadrant photo diode. The light is collimated via the appendant high NA condenser, reflected by another dichroic mirror and corrected for slight tilt misalignment by a telescope, which reduces the diameter

to match the quadrant photo diode.

Methods

Back-focal plane detection

Positional detection with high scan rates ($> \text{kHz}$ and $< 10 \text{ nm}$) can be achieved by imaging the back-focal plane of the condenser onto a quadrant photo-diode (QPD) or a position sensitive diode. The back-focal plane is conjugate to the object plane. That means that we do not image the object but its fourier transform. In our case, a bead near the focus of the laser beam will act as a scatterer and the interference pattern of the scattered and the unscattered laserlight is relayed to the QPD. As its name suggests it is divided into four quadrants and minute shifts of intensity result in large signals when comparing e.g. the left two quadrants against the right ones.

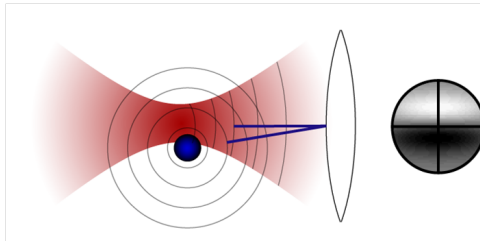


Figure 4: The trapped particle acts as a scattering center. Interference with the unscattered light creates a characteristic intensity profile at the back-focal plane that is relayed to the QPD.

Equipartition theorem

Our particle undergoes thermal motion in the optical trap. The principle of equipartition of energy states that then the mean energy per degree of freedom is $\langle U \rangle = \frac{1}{2}k_B T$. By degree of freedom is meant, that we can calculate the energy from its position in all three dimensions – its three degrees of freedom – (more precisely their squares) and these simply add up to the total energy. We now consider the energy in one dimension as $U(x) = \frac{1}{2}\kappa x^2$ and average

$$\langle U(x) \rangle = \frac{1}{2}\kappa \langle x^2 \rangle = \frac{1}{2}k_B T. \quad (11)$$

Depending on the actual trap stiffness we need 10^5 data points to obtain a smooth distribution. Note, that it might be advantageous to fit the normal distribution instead of directly calculating $\langle x^2 \rangle$.

Auto-correlation and power spectral density³

The auto-correlation of a signal $x(t)$ with time lag τ is defined as

$$R_x(\tau) = \langle x(t)x(t - \tau) \rangle. \quad (12)$$

³This discussion shows the definitions presented in [2] and follows the treatment in [3]

A high value of the auto-correlation signifies that the particle “remembers” where it has been. When it approaches zero it means that the former position does not influence its current position anymore. A freely moving particle will remain in a small area for some time (high auto-correlation for small τ) and eventually diffuse out of this area after longer times (low or no auto-correlation for longer times).

Similar information is represented in the power spectral density, PSD, which is defined as the as the Fourier transform of the autocorrelation

$$G_x(f) = \mathfrak{F}\{R_x(\tau)\} = \int_{-\infty}^{\infty} d\tau e^{2\pi i f \tau} \langle x(t)x(t-\tau) \rangle_t. \quad (13)$$

Each interval $G_x(f)\Delta f$ corresponds to the contribution of an oscillation of frequency f to the signal, that is a cosine signal would only contribute a single peak to the power spectral density. For finite measurement time T and sampling rate f_s the power spectral density is symmetric about the Nyquist frequency $f_{Ny} = f_s/2$. The so-called one-sided PSD therefore folds this second half of the back onto itself and is normalized by the measurement time

$$P(f) = \frac{2 \langle |\hat{x}|^2 \rangle}{T}. \quad (14)$$

In order to extract information from the PSD we need a model that connects the motion of the bead in the – to first order – harmonic potential of the optical trap. Its equation of motion reads

$$m\ddot{x}(t) + \gamma\dot{x}(t) + \kappa x(t) = \gamma\sqrt{2D}\xi(t), \quad (15)$$

where the drag coefficient $\gamma = 6\pi\eta R$ relates the force onto a bead of radius R in a medium of viscosity η to its velocity \dot{x} . κ is the spring constant of our trap potential and $\xi(t)$ are random, thermal forces on the bead. Their exact prefactor originates in the Einstein relation. These exhibit zero mean, $\langle \xi(t) \rangle = 0$, and are uncorrelated, $\langle \xi(t)\xi(t') \rangle = \delta(t-t')$, which translates into a flat PSD with magnitude proportional to the measurement time T . This is a so-called Langevin equation. We introduce the corner frequency $f_c = \frac{\kappa}{2\pi\gamma}$. Its reciprocal $\frac{\gamma}{\kappa}$ gives a time scale on which each thermal collision has been dissipated. For our overdamped system we can drop the inertia term and the equation of motion now reads

$$\dot{x}(t) + 2\pi f_c x(t) = \sqrt{2D}\xi(t). \quad (16)$$

In order to calculate the PSD later on, we Fourier transform it term by term

$$\mathfrak{F}\{2\pi f_c x(t)\} = 2\pi f_c \hat{x}(f) \quad (17)$$

$$\mathfrak{F}\{\sqrt{2D}\xi(t)\} = \sqrt{2D}\hat{\xi}(f) \quad (18)$$

$$\mathfrak{F}\{\dot{x}(t)\} = \int_{-\infty}^{\infty} dt e^{2\pi i f t} \dot{x}(t) \quad (19)$$

$$= \underbrace{[x(t)e^{2\pi i f t}]_{-\infty}^{\infty}}_{\text{neglected}} - 2\pi i f \underbrace{\int_{-\infty}^{\infty} dt e^{2\pi i f t} x(t)}_{\hat{x}(f)} \quad (20)$$

Rearranging gives the fourier transform of $x(t)$

$$\hat{x}(f) = \frac{\sqrt{2D}\hat{\xi}(f)}{2\pi(f_c - if)}, \quad (21)$$

which we use to calculate the PSD according to equation 14

$$P(f) = \frac{D}{2\pi^2T} \frac{\langle |\hat{\xi}(f)|^2 \rangle}{f_c^2 + f^2}. \quad (22)$$

For finite measurement time we can evaluate the noise term to T and, finally, the power spectral density of a particle undergoing one-dimensional Brownian motion in an harmonic potential (and luckily the motion decouples into the two or three directions) is

$$P(f) = \frac{2D}{\pi^2(f_c^2 + f^2)}. \quad (23)$$

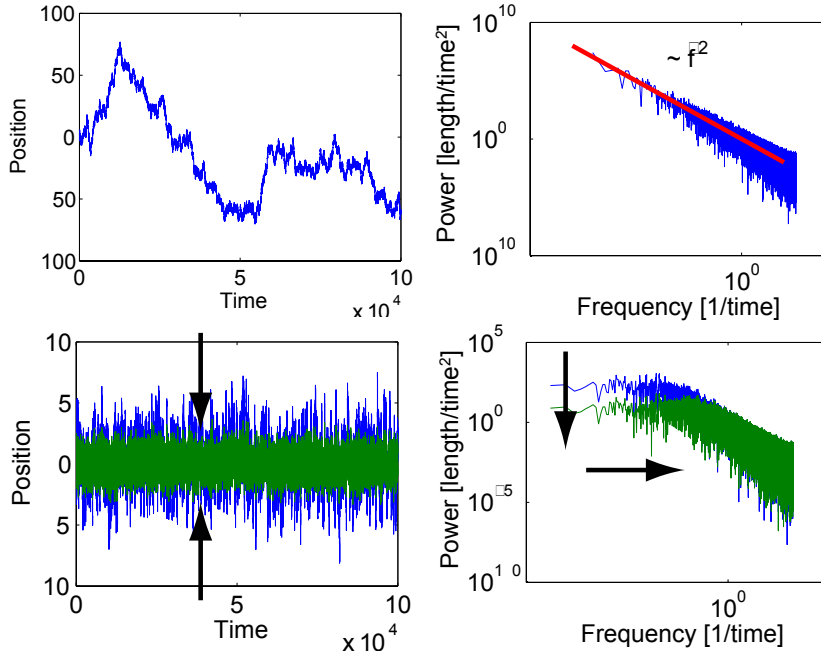


Figure 5: *Upper panels:* The top left panel shows the position signal of a particle undergoing unrestricted Brownian motion. The power spectral density of the signal shows the characteristic $\propto 1/f^2$ behavior at the right. *Lower Panels:* The left panel shows the position signal of a particle undergoing Brownian motion in two potentials with different trap stiffness. The motion is now restricted, the higher κ the more constricted it is. In the power spectral densities this is reflected by a shift of the corner frequency f_c to higher frequencies. That means that the particle feels the confining potential already at shorter time scales.

Tasks

Back-focal plane detection: Map the position signal from the QPD.

Thermal motion: Measure the thermal motion of polystyrene beads in the optical trap for different laser powers and bead sizes.

Equipartition theorem: Calculate the trap stiffness of the optical tweezers setup for different laser powers and bead sizes via the equipartition theorem.

Power spectral density: Calculate the trap stiffness of the optical tweezers setup for different laser powers and bead sizes via the power spectral density of the position signal.

Viscosity: Calculate the viscosity of the solution in the sample.

Error discussion: Discuss limitations and possible sources of error.

Procedure

Laser power: Measure the laser power after the objective with respect to the amplifier current of the laser. Allow the laser to warm up for 20 minutes at high amplifier current setting and measure by successively lowering it.

Field of view: Put grating slide with scale bar on microscope. Make a snapshot with the CCD-camera and determine the field of view (use IrfanView, Photoshop or alike). Draw scale bar five times and calculate error.

Bead size: Make snapshots of five beads of each sample provided and evaluate their size by using the previously found scale. Include error calculation.

QPD map: Use the piezo stage to move a stuck bead across the laser focus in defined steps and record the position signal from the QPD (*Plot for one bead size*). Use this data to determine the linear range of the detector and the conversion factor. Compare it for each bead size.

Thermal motion: Trap a bead and measure its thermal motion of a trapped bead for a around ten seconds at 10 – 20 kHz at 5 decreasing laser powers (*Plot for one size*).

Different sizes: Repeat beads with different sizes. Mind the changing conversion factor.

Trap stiffness: Compare the results of the two different methods. Relate bead size, laser power and trap stiffness (*Plot*) and discuss the results.

Viscosity: Use this data to determine the viscosity of the sample solutions. Relate it to the laser power and discuss the results.

Error discussion: Discuss limitations and possible sources of error.

Bibliography

- [1] K Svoboda and S M Block. Biological applications of optical forces. *Annual Review of Biophysics and Biomolecular Structure*, 23:247–285, 1994. PMID: 7919782.
- [2] J. Howard. *Mechanics of Motor Proteins and the Cytoskeleton*. Sinauer Associates, Inc., Sunderland, 2001.
- [3] Kirstine Berg-Sørensen and Henrik Flyvbjerg. Power spectrum analysis for optical tweezers. *Review of Scientific Instruments*, 75(3):594, 2004.